Transp Porous Med (2007) 70:355–373
DOI 10.1007/s11242-007-9104-9

ORIGINAL PAPER

Heat and brine transport in porous media: the Oberbeck-Boussinesq approximation revisited

Anke Jannie Landman · Ruud J. Schotting

Received: 2 August 2006 / Accepted: 17 January 2007 / Published online: 23 March 2007

Abstract This paper discusses the Oberbeck-Boussinesq approximation for heat and solute transport in porous media. In this commonly used approximation all density variations are neglected except for the gravity term in Darcy's law. However, in the limit of vanishing density differences this gravity term disappears as well. The main purpose of this paper is to give the correct limits in which the gravity term is retained, while other density effects can be neglected. We show that for isothermal brine transport, fluid volume changes can be neglected when a condition is fulfilled for a dimensionless number, which is independent of the density difference and specific discharge. For heat transfer an additional condition is required. One-dimensional examples of simultaneous heat and brine transport are given for which similarity solutions are constructed. These examples are included to elucidate the volume effects and the corresponding induced specific discharge variations. Finally, a two-dimensional example illustrates the relative effects of volume changes and gravity.

Keywords Oberbeck-Boussinesq approximation · Heat transfer · Brine transport · Solute transport · Similarity transformations · Density-dependent flow · Porous media

A.J. Landman
Improved Oil Recovery and Water Management, Shell International Exploration and Production B.V., Kesslerpark 1, 2288 GS Rijswijk, The Netherlands
e-mail: anke.landman@shell.com

R.J. Schotting (✉)
University of Utrecht, Department of Earth Sciences, Environmental Hydrogeology Group, P.O. Box 80021, 3508 TA Utrecht, The Netherlands
e-mail: schotting@geo.uu.nl

1 Introduction

The Oberbeck-Boussinesq approximation is a widely used and powerful simplification in studies of density-dependent flows. In the literature, this approximation is commonly named after Boussinesq (Boussinesq, 1903), though Oberbeck (Oberbeck, 1879) was the first scientist who made use of it. The approximation in its strictest form includes the following four assumptions (Gartling and Hickox, 1985; Joseph, 1976; Gray and Giorgini, 1976):

1. Density variations - induced by variations in temperature and/or solute concentration - are neglected in all equations, with the exception of the gravity term in the equation of motion.
2. All other material properties (e.g. viscosity, heat capacity, thermal conductivity, solute molecular diffusivity) are assumed constant.
3. Viscous dissipation is assumed negligible.
4. The equation of state is linearized.

Different versions and extensions of the Oberbeck-Boussinesq approximation are in use. For instance, Gartling and Hickox (Gartling and Hickox, 1985) employ the so-called "relaxed" or "extended" Boussinesq approximation, in which fluid properties other than density are allowed to vary.

The present study only focuses on the first and most important assumption. Most researchers state that this assumption is valid in cases where density variations are small. However, in the limit of density differences approaching zero, the governing equations do not reduce to those used in the Boussinesq approximation. In this limit, the gravitational term in the equation of motion vanishes as well. In many practical cases, such as problems involving the intrusion of sea water or storage of thermal energy in aquifers, gravity can play an important role. In those cases the Boussinesq approximation often works well. In the words of Daniel Joseph (Joseph, 1976): "... there is no special reason, besides our lack of proofs, to doubt the validity of the Oberbeck-Boussinesq equations in some limit of small parameters."

Numerous researchers have tried to derive the Boussinesq equations for ordinary fluids. See for example Rajagopal et al. (Rajagopal et al. 1996) who give a short overview of the different approaches. For fluids in porous media, the validity of the Boussinesq approximation was tested numerically by various authors (Gartling and Hickox, 1985; Leijnse, 1989; Peirotti et al. 1987; Johannsen, 2003). The present paper deals with the Boussinesq approximation in a different way. An attempt is made to give the formal limits in which the Boussinesq equations for transport in porous media are obtained. This is done by deriving explicit equations for the relative changes in fluid volume. These volume changes are neglected in the Boussinesq approximation, yielding the continuity equation in its incompressible form: $\nabla \cdot \mathbf{q} = 0$. Three cases are discussed: isothermal brine transport, heat transfer in fresh water, and simultaneous transport of heat and brine.

In the second part of the paper some examples are given to illustrate the effect of volume changes and adopting the Boussinesq approximation. For two one-dimensional examples of simultaneous heat and brine transport similarity solutions were constructed, based on the fully coupled equations. In addition to these semi-analytical solutions numerical solutions are given for comparison. The similarity solutions may be useful for computer code verification with regard to simultaneous transport of heat

and solute in porous media. Finally, the Boussinesq approximation is discussed for a two-dimensional example in which gravity plays an important role.

2 Governing equations

This section presents the standard set of equations for salt and heat transport in a rigid, homogeneous, isotropic porous medium. The five governing equations are: the mass balances of the fluid and the salt, the energy balance, Darcy's law, and an equation of state that relates the fluid density to the temperature and the salt mass fraction.

Fluid mass balance

$$n\frac{\partial \rho}{\partial t} + \nabla \cdot (\rho \mathbf{q}) = 0, \tag{1}$$

where ρ denotes the fluid density, n the porosity and $\mathbf{q}$ the specific discharge vector.

Salt mass balance

$$n\frac{\partial (\rho\omega)}{\partial t} + \nabla \cdot (\rho \mathbf{q}\omega - \mathbf{D}\rho\nabla\omega) = 0, \tag{2}$$

where ω is the salt mass fraction and $\mathbf{D}$ is the diffusion/dispersion tensor. The salt mass fraction (a dimensionless variable) is defined as the ratio of salt concentration to fluid density.

Energy balance

$$nc_{\mathrm{f}}\frac{\partial (\rho T)}{\partial t} + (1-n)\rho_{\mathrm{s}}c_{\mathrm{s}}\frac{\partial T}{\partial t} + \nabla \cdot (c_{\mathrm{f}}\rho \mathbf{q}T - \lambda_{\mathrm{eff}}\nabla T) = 0, \tag{3}$$

where c_{f} and c_{s} denote the specific heat of fluid and solid (soil particles), respectively. Moreover, T is the temperature and λ_{eff} the effective thermal conductivity of the porous medium. This equation assumes thermal equilibrium between the fluid and solid phases.

Darcy's law

$$\mathbf{q} + \frac{k}{\mu}(\nabla p - \rho \mathbf{g}) = 0, \tag{4}$$

where p denotes the fluid pressure, k the intrinsic permeability, μ the dynamic fluid viscosity and $\mathbf{g}$ the acceleration of gravity.

Equation of state

$$\rho = \rho_0 e^{\gamma\omega - \alpha(T - T_0)}, \tag{5}$$

where ρ_0 and T_0 are the reference density and the reference temperature, γ is the coefficient of volume expansion due to the presence of salt in the fluid ($\gamma \approx 0.692$), and α is the thermal expansion coefficient of the fluid.

Using the equation of state (5) to eliminate the salt mass fraction in (2), and combining the fluid mass balance (1) with (3) and (2) yields for the salt mass and energy balances:

$$n\frac{\partial \rho}{\partial t} + n\alpha\rho\frac{\partial T}{\partial t} + \mathbf{q} \cdot \nabla\rho + \alpha\rho\mathbf{q} \cdot \nabla T - \nabla \cdot (\mathbf{D}\nabla\rho + \alpha\mathbf{D}\rho\nabla T) = 0, \tag{6}$$

$$(nc_f\rho + (1-n)\rho_s c_s)\frac{\partial T}{\partial t} + c_f\rho\mathbf{q}\cdot\nabla T - \nabla\cdot(\lambda_{\text{eff}}\nabla T) = 0. \tag{7}$$

Equations (1), (4), (6), and (7) form the set of coupled nonlinear partial differential equations that is the starting point of the analysis in this paper. Next, the equations are scaled using:

$$\rho^* = \frac{\rho-\rho_0}{\rho_{\max}-\rho_0}, \quad T^* = \frac{T-T_{\min}}{T_0-T_{\min}}, \quad \rho^* = \frac{pk}{\mu q_0 x_0}, \quad \text{and} \quad \omega^* = \frac{\omega}{\omega_{\max}}, \tag{8}$$

where $T_{\min}$, $\rho_{\max}$, and $\omega_{\max}$ denote the minimum temperature and the maximum density and salt mass fraction. Note that the reference density ρ_0 is the minimum density in the example problems that will be discussed. This density corresponds to the maximum temperature (reference temperature T_0) and a zero salt mass fraction. With the use of (8), the temperature, density, and mass fraction are scaled to have values between zero and one. Furthermore, the specific discharge and space and time variables are rendered dimensionless by introducing a characteristic discharge q_0 and characteristic length x_0:

$$\mathbf{q}^* = \frac{\mathbf{q}}{q_0}, \quad \mathbf{x}^* = \frac{\mathbf{x}}{x_0}, \text{ and } t^* = \frac{tq_0}{nx_0}. \tag{9}$$

Moreover, the following dimensionless coefficients are introduced:

$$N = \frac{k\rho_0 g}{\mu q_0}, \quad A = \frac{(1-n)\rho_s c_s}{n\rho_0 c_f}, \quad \alpha^* = \alpha(T_0 - T_{\min}), \text{ and } \gamma^* = \gamma\omega_{\max}. \tag{10}$$

Note that N resembles the gravity number ($\mathrm{N_g} = \mathrm{Ra/Pe}$, where $\mathrm{Ra} = kgx_0(\rho_{\max}-\rho_0)/(\mu D)$), with the difference that N contains the absolute reference density instead of the density difference. A incorporates the effect of thermal retardation caused by heat storage in the solid phase.

The Péclet number expresses the ratio of convective transport to molecular diffusion. In addition, the ratio of thermal diffusion to solute diffusion is needed, the Lewis number:

$$\mathrm{Pe} = \frac{q_0 x_0}{D}, \text{ and } \mathrm{Le} = \frac{\lambda}{\rho_0 c_f D} = \frac{a}{D}, \tag{11}$$

where a is the effective thermal diffusion coefficient. For the moment, velocity-dependent dispersion is disregarded and it is assumed that λ_{eff} and D are constants. The last parameter that is introduced is the one that describes the maximum relative density difference in a specific density-dependent flow problem. This important parameter is given by:

$$\varepsilon = \frac{\rho_{\max}-\rho_0}{\rho_0}. \tag{12}$$

The resulting set of dimensionless equations is given by (omitting the asterisks notation for convenience):

$$\varepsilon\frac{\partial\rho}{\partial t} + \nabla\cdot[(1+\varepsilon\rho)\mathbf{q}] = 0, \tag{13}$$

$$\begin{aligned}\varepsilon\frac{\partial\rho}{\partial t} &+\alpha(1+\varepsilon\rho)\frac{\partial T}{\partial t} + \varepsilon\mathbf{q}\cdot\nabla\rho + \alpha(1+\varepsilon\rho)\mathbf{q}\cdot\nabla T \\ &-\frac{\varepsilon}{\mathrm{Pe}}\Delta\rho - \frac{\alpha}{\mathrm{Pe}}\nabla\cdot[(1+\varepsilon\rho)\nabla T] = 0,\end{aligned} \tag{14}$$

$$(1+\varepsilon\rho+A)\frac{\partial T}{\partial t}+(1+\varepsilon\rho)\mathbf{q}\cdot\nabla T-\frac{\mathrm{Le}}{\mathrm{Pe}}\Delta T=0, \tag{15}$$

$$\mathbf{q}+\nabla p+N(1+\varepsilon\rho)\vec{e}_z=0, \tag{16}$$

where $\vec{e}_z$ denotes the unit vector in the z-direction. The scaled version of the equation of state is given by:

$$\rho=\frac{1}{\varepsilon}\left(e^{\gamma\omega-\alpha(T-1)}-1\right). \tag{17}$$

As observed by Joseph (Joseph, 1976), the formal limit $\varepsilon\downarrow 0$ in (13)–(16) does not yield equations consistent with the Boussinesq approximation. In this limit, the density effects vanish from all equations, including Darcy's law. However, in the Boussinesq approximation the density dependency in Darcy's law is retained.

3 The Boussinesq limit revisited

In this section we investigate the limits in which the equations are obtained as in the Boussinesq approximation. Three cases are discussed: isothermal brine transport, heat transfer in fresh water, and simultaneous transport of heat and brine.

3.1 Isothermal brine transport

The scaled equations for the case of isothermal brine transport are given by (13), (14), and (16). Note that under isothermal conditions, (14) reduces to:

$$\frac{\partial\rho}{\partial t}+\mathbf{q}\cdot\nabla\rho-\frac{1}{\mathrm{Pe}}\Delta\rho=0. \tag{18}$$

Expanding the divergence term in (13), and subtracting (18) multiplied by ε from this yields (after rearranging terms):

$$\nabla\cdot\mathbf{q}=-\frac{\varepsilon}{\mathrm{Pe}(1+\varepsilon\rho)}\Delta\rho. \tag{19}$$

Taking the divergence of (16) and substituting (19) in the result gives the elliptic pressure equation:

$$\Delta p=\underbrace{\frac{\varepsilon}{\mathrm{Pe}(1+\varepsilon\rho)}\Delta\rho}_{\text{Volumechanges}}-\underbrace{N\varepsilon\frac{\partial\rho}{\partial z}}_{\text{Gravity}}. \tag{20}$$

Note that both terms in (20) contain the relative density difference ε. It is generally said that volume changes can be neglected for small density differences, i.e. small ε. This is true, but at the same time the second term in (20) becomes small when $\varepsilon\downarrow 0$. Disregarding the volume changes but retaining the gravity term can only be done when $N\mathrm{Pe}\gg 1$. Note that this condition is independent of ε:

$$N\mathrm{Pe}=\frac{kg\rho_0x_0}{\mu D}=\frac{\mathrm{Ra}}{\varepsilon}. \tag{21}$$

The role of the diffusion coefficient can be explained as follows. When for example two equal volumes of a high and a low salt concentration are added, eventually the

concentration will distribute itself evenly due to molecular diffusion. The resulting total volume is slightly smaller than the sum of the two volumes. In the hypothetic case of zero molecular diffusion, no mixing would occur at all when the two volumes are added, and no change in fluid volume would take place. Therefore, when the diffusion coefficient is very small, Pe is large and the condition $N\text{Pe} \gg 1$ will easily be satisfied.

The other parameters in $N\text{Pe} \gg 1$ are fixed (g), medium (k), or fluid (ρ_0, μ) properties, except for x_0. When the characteristic length x_0 of interest is small, volume effects are relatively more important than for larger lengths. The effect of volume changes on the flow field is a local phenomenon, taking place at the location where high density gradients occur. This will be illustrated with the examples in Section 4.1.

Finally we recast the transport equation (18), by rewriting it in terms of the salt mass fraction ω, using (17) with $T =$ constant. Without any further assumptions, the following equation is obtained:

$$\frac{\partial \omega}{\partial t} + \mathbf{q} \cdot \nabla \omega - \frac{1}{\text{Pe}} \Delta \omega = \frac{\gamma}{\text{Pe}} (\nabla \omega)^2. \tag{22}$$

In the Boussinesq approximation, (22) is used with the difference that the right hand side is zero. This would be obtained from the original salt mass balance (2) directly, under the assumption of a constant density. However, the constant density assumption would also imply neglecting the gravity term in (20). The constant density assumption therefore does not agree with the Boussinesq approximation. To obtain the transport equation as it is in the Boussinesq approximation, the right hand side of (22) should be small enough to be neglected, in comparison with the other terms in (22). When the gradient of ω is small (but not zero), the second order term on the right hand side will be small compared to the other terms. In addition, when $\gamma\omega \ll 1$, the equation of state (17) can be linearized to $\rho = \gamma/\omega\varepsilon$, yielding the desired transport equation directly from (18). This linearization is often done (see point 4 in the Introduction), but not strictly necessary.

3.2 Heat transfer in fresh water

In this section only heat transfer is considered, which is described by equations (13), (15), and (16). The equation of state (17) is used to write (13) in terms of the temperature. Note that the salt mass fraction is omitted in the equation of state because fresh water is considered. Combining (13) and (15) yields:

$$\nabla \cdot \mathbf{q} = \frac{\alpha}{1 + \varepsilon\rho + A} [A\mathbf{q} \cdot \nabla T + \frac{\text{Le}}{\text{Pe}} \Delta T], \tag{23}$$

or, with the right-hand side of (23) written in terms of the density only:

$$\nabla \cdot \mathbf{q} = -\frac{1}{1 + \varepsilon\rho + A} \left[\frac{\varepsilon A}{1 + \varepsilon\rho} \mathbf{q} \cdot \nabla \rho + \varepsilon \frac{\text{Le}}{\text{Pe}} \nabla \cdot \left(\frac{1}{(1 + \varepsilon\rho)} \nabla \rho \right) \right]. \tag{24}$$

Finally, after combining (24) and (16), we obtain for the Laplacian of the fluid pressure:

$$\Delta p = \underbrace{-\frac{1}{1 + \varepsilon\rho + A} \left[\overbrace{\frac{\varepsilon A}{1 + \varepsilon\rho} \mathbf{q} \cdot \nabla \rho}^{\text{Heat convection}} + \overbrace{\varepsilon \frac{\text{Le}}{\text{Pe}} \nabla \cdot \left(\frac{1}{(1 + \varepsilon\rho)} \nabla \rho \right)}^{\text{Heat conduction}} \right]}_{\text{Fluid volume changes}} + \underbrace{N\varepsilon \frac{\partial \rho}{\partial z}}_{\text{Gravity}}. \tag{25}$$

Note that in Section 2 the Péclet number was defined for solute transport. As a consequence, the ratio of Le and Pe appears in the heat transfer equations. This ratio is nothing else than the reciprocal of Pe defined for heat transfer ($\mathrm{Pe_T} = q_0 x_0 \rho_0 c_\mathrm{f}/\lambda_\mathrm{eff}$).

In comparison with the case of isothermal brine transport, the situation is now slightly more complicated. The term in (25) that accounts for fluid volume changes consists of two parts: a convective term (due to the heat capacity of the solid grains) and a diffusive term (due to effective heat conduction). Hence, the limit $\mathrm{Le}/\mathrm{Pe} \ll N$ in (25) is not sufficient. In this limit, only the diffusive term vanishes, while the convective term remains unaffected. To be able to disregard all volume changes and retain the gravity term, the condition $|\mathbf{q}| \ll N$ must be fulfilled as well (A and $(1+\varepsilon\rho)$ being of order 1).

In one sense, the convective term in (25) plays a peculiar role. To elucidate its consequences, the following one-dimensional heat convection problem is considered: let $\mathrm{Le} = 0$, i.e. no heat conduction, while the initial temperature distribution is given by $T(x,0) = T_\mathrm{i}(x)$, corresponding to $\rho(x,0) = \rho_\mathrm{i}(x)$, and $q(-\infty,t) = q_\mathrm{L}$. For this particular case equation (15) reduces to:

$$\frac{\partial \rho}{\partial t} + \frac{(1+\varepsilon\rho)q}{(1+\varepsilon\rho+A)}\frac{\partial \rho}{\partial x} = 0, \tag{26}$$

and combining (13) and (15) yields:

$$\frac{\partial q}{\partial x} = -\frac{\varepsilon A q}{(1+\varepsilon\rho+A)(1+\varepsilon\rho)}\frac{\partial \rho}{\partial x}. \tag{27}$$

This is the 1D version of equation (24), without the conductive term. Integration of (27) yields:

$$q = \frac{(1+\varepsilon\rho+A)}{(1+\varepsilon\rho)}C. \tag{28}$$

Substitution in (26) gives:

$$\frac{\partial \rho}{\partial t} + C\frac{\partial \rho}{\partial x} = 0, \tag{29}$$

where C is a constant that can be determined by applying the boundary conditions for q and ρ at $x = -\infty$. For example, when $\rho(-\infty,t) = 1$, then $C = q_\mathrm{L}(1+\varepsilon)/(1+\varepsilon+A)$.

Due to the hyperbolic character of (29), the initial temperature/density distribution moves with a constant speed C, without changing shape, even though the specific discharge q is non-uniform. In the limit $\varepsilon \downarrow 0$ a constant front velocity $C = q_\mathrm{L}/(1+A)$ is obtained. Hence, the difference between this limit and the exact equations is a small change in the front velocity of order ε. However, if a divergence free discharge is assumed, like in the Boussinesq approximation, the density distribution does change in shape, the front velocity being non-uniform. In this case the front velocity depends on the density distribution and equals $q_\mathrm{L}(1+\varepsilon\rho)/(1+\varepsilon\rho+A)$.

3.3 Simultaneous heat and brine transport

This section discusses the transport of both heat and brine. The governing equations are given in their scaled form by (13)–(16). Combining (13) and (14) gives an expression for $\nabla \cdot \mathbf{q}$ in terms of ρ and T. Eliminating the time dependent term using (15) results in the following expression:

$$\nabla \cdot \mathbf{q} = \frac{\alpha(\mathrm{Le}/\mathrm{Pe})\Delta T + \alpha A \mathbf{q} \cdot \nabla T}{1 + \varepsilon\rho + A} - \frac{\varepsilon \Delta\rho}{\mathrm{Pe}(\varepsilon\rho + 1)} - \frac{\alpha}{\mathrm{Pe}(\varepsilon\rho + 1)} \nabla \cdot ((\varepsilon\rho + 1)\nabla T). \tag{30}$$

This expression can be compared to equations (19) and (23), the separate cases of brine transport and heat transport. The first term in (30) is equal to (23). It expresses the contribution of temperature gradients to the changes in fluid volume. The remaining part of (30) seems to contain an extra term compared to equation (19). However, $\Delta\rho$ in (19) contains the effect of concentration only, whereas $\Delta\rho$ in (30) accounts for temperature differences as well. When $\Delta\rho$ in (30) is expressed in terms of ω and T using the equation of state (17), the part that depends on the temperature cancels out the last term. Consequently, the remaining part of (30) is equal to (19). This means that the fluid volume changes in a problem that considers transport of both heat and brine are simply a summation of the fluid volume changes caused by the two separate effects.

Combining (30) with the equation of motion (16) would yield an expression similar to (25) with the fluid volume changes given by (30). To obtain the equations in the Boussinesq approximation, the conditions for the separate cases of heat and brine transport must both be fulfilled.

4 Examples

First we discuss two one-dimensional examples of simultaneous heat and brine transport, for which similarity solutions are presented. These examples are meant to illustrate the local enhancement or reduction of the specific discharge as a result of volume changes, the effect that is neglected under the Boussinesq approximation. Due to the one dimensionality, gravity does not play a role in these cases. Finally we will present a two-dimensional example of brine transport in a heterogeneous medium. This example illustrates the effects of both the gravity term and volume changes.

4.1 1D simultaneous heat and mass diffusion

We solve the complete system of equations for two one-dimensional examples of simultaneous heat and brine transport. Both problems initially have a discontinuity in the density at $x = 0$, caused by discontinuities in the temperature and salt mass fraction. The initial conditions for problem I are (scaled variables):

$$\begin{aligned} T = 0 \ \text{ and } \ \omega = 1 \quad \text{for } \ x < 0, \\ T = 1 \ \text{ and } \ \omega = 0 \quad \text{for } \ x > 0. \end{aligned} \tag{31}$$

So, for negative x the temperature and salt mass fraction equal their minimum and maximum values respectively, resulting in the maximum density possible. For positive x the density equals its minimum value. In problem II the initial profile of the salt mass fraction is reversed:

$$\begin{aligned} T = 0 \text{ and } \ \omega = 0 \quad \text{for } \ x < 0, \\ T = 1 \text{ and } \ \omega = 1 \quad \text{for } \ x > 0. \end{aligned} \tag{32}$$

Table 1 Dimensionless parameters

γ	0.076
α	0.02
A	1
Le	400
Pe	0.1

Whereas in problem I the temperature and mass fraction distributions have an enhancing effect on the density, they have an opposing effect in problem II.

The specific discharge q is chosen to be zero at infinity for all times:

$$q = 0 \quad \text{for } x \to \infty. \tag{33}$$

For these two cases, semi-analytical solutions were constructed with the use of similarity transformations. This method is described in the Appendix. In addition, the problems were solved numerically. The similarity solutions are not fully analytical, as a numerical method was also necessary to solve the resulting set of ordinary differential equations (50)–(52). What is referred to as the numerical solution here, was obtained by numerical integration of the original equations (13)–(15), using finite differences. A solution at a certain time t can be compared to the similarity solution, because every x corresponds to an η according to (41): $\eta = x/\sqrt{t}$.

Table 1 displays the values that were used for the five non-dimensional variables involved. The value for α corresponds to a temperature difference of 60°C, the value for γ corresponds to a maximum salt mass fraction of 0.11. These values yield a maximum relative density difference ε of 0.1, which is approximately half that of fully saturated brine.

Figures 1 and 2 show the scaled density and temperature profiles for problem I and II respectively. In both figures, the profiles obtained with the different methods are indistinguishable. This perfect match is not found for very short or long times. The reason for this is that the boundary and initial conditions used to obtain the numerical solution are somewhat different from the exact ones defined in (31)–(33). One difference is that the spatial domain used in the calculations is finite instead of infinite. Another difference is that the discontinuities in the initial profiles are approximated by steep error functions. Therefore, for short times the numerical solution depends on the quality of this approximation and differs from the similarity solution. This effect decreases with increasing time. On the other hand, for long times relative to the size of the domain, the numerical solution starts to deviate from the similarity solution because of the influence of the boundaries.

Figures 3 and 4 show the specific discharge profiles for the two problems. The non-zero discharge is a result of the fluid volume changes due to variations in salt mass fraction and temperature (see (30)). Again the two solutions coincide. Note that the magnitude of the specific discharge enhancement reduces in time with $1/\sqrt{t}$.

The separate contributions of the gradients in temperature and salt mass fraction become apparent in comparing Figures 3 and 4. It can be seen that the narrow peak is caused by the salt mass fraction gradient, since this gradient is the one that is reversed in problem II. The change in the specific discharge caused by the temperature gradient spans a much wider region. The transition zone for the temperature is wider than that for the salt mass fraction, thermal diffusion having a much greater magnitude than salt mass diffusion (Le = 400).

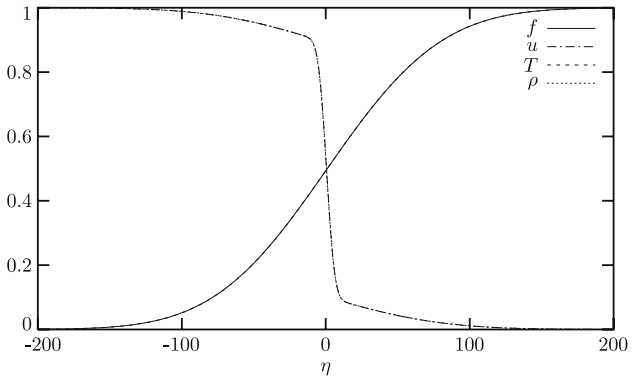

Fig. 1 Computed temperature and density profiles for problem I. Similarity solutions f and u compared to numerical solutions T and ρ

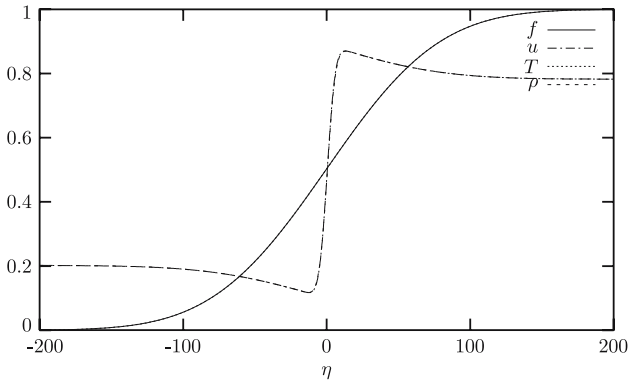

Fig. 2 Computed temperature and density profiles for problem II. Similarity solutions f and u compared to numerical solutions T and ρ

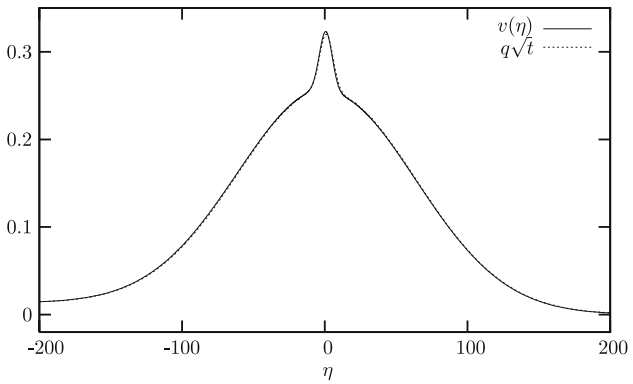

Fig. 3 Computed specific discharge for problem I. The similarity solution $v(\eta)$ compared to the numerical solution $q\sqrt{t}$

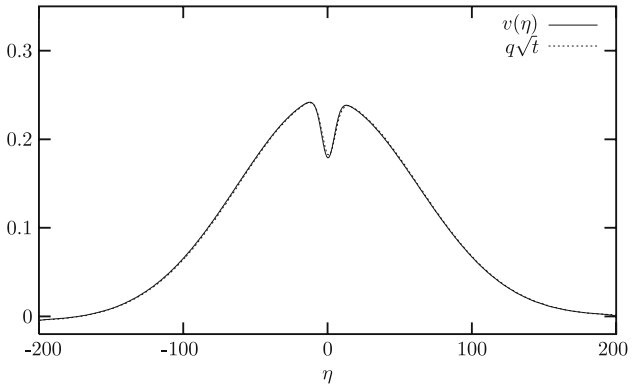

Fig. 4 Computed specific discharge for problem II. The similarity solution $v(\eta)$ compared to the numerical solution $q\sqrt{t}$

The asymmetry in the discharge profiles - note the non-zero discharges for $\eta \to -\infty$ in Figures 3 and 4 - is caused by the $\varepsilon\rho$ term in the denominators of equations (19), (23) and (30). Increasing the value of ε amplifies this asymmetry and also the magnitude of the specific discharge enhancement. However, the value of $\varepsilon(= \exp(\gamma + \alpha) - 1)$ has little effect on the shape of the solutions that are presented in Figures 1 and 2. They are mainly determined by the ratio of γ and α, in other words, by the relative contributions of salt mass fraction and temperature to the maximum density difference. In addition, the solutions depend on the Lewis and Péclet numbers, for which we aimed to use realistic values. The next paragraph discusses the choice of the characteristic length and discharge that determine the value of the Péclet number.

4.1.1 The characteristic length and discharge

In Section 2, a characteristic length x_0 and discharge q_0 were introduced to render the equations fully non-dimensional. These characteristic variables also appear in the Péclet number. It is common to use a characteristic length scale that is related to the size of the macroscopic domain. As a characteristic value for the specific discharge the background flow can be used. However, a background flow was absent in the example problems discussed previously. For these cases we suggest the following approach.

The flow in the example problems is caused purely by fluid volume changes. For one-dimensional transport of solute this is expressed by the following equation:

$$\frac{\partial q}{\partial x} = -\frac{D}{\rho}\frac{\partial^2 \rho}{\partial x^2}, \tag{34}$$

which is the one-dimensional unscaled version of (19). The characteristic velocity is therefore related to the diffusion constant and the density gradient:

$$q_0 \sim \frac{D\nabla\rho}{\rho_0}. \tag{35}$$

The density gradient can be approximated by the maximum density difference divided by the length scale in which the change in density occurs. This length scale at the same

time serves as the characteristic length. It is the penetration depth of a diffusion problem:

$$x_0 \sim \sqrt{Dt}. \tag{36}$$

With this the characteristic velocity becomes:

$$q_0 \sim \frac{D(\rho_{\max} - \rho_0)}{\rho_0 \sqrt{Dt}} = \varepsilon \sqrt{\frac{D}{t}}. \tag{37}$$

When these characteristic scales are incorporated in the Péclet number, the following is found:

$$\mathrm{Pe} = \frac{x_0 q_0}{D} \sim \varepsilon. \tag{38}$$

Therefore, ε was used as the value of the Péclet number in the two example problems.

4.1.2 Hydrodynamic dispersion

So far, the thermal and molecular diffusivities were treated as constants. The ratio of the two diffusivities was given by Le, for which a realistic value was chosen in the examples discussed. The effect of hydrodynamic dispersion was disregarded. In the absence of a background flow this is a reasonable assumption. For a non-zero background flow, however, a larger value for the diffusion/dispersion coefficient should be chosen to account for hydrodynamic dispersion. Commonly, this coefficient is a function of the velocity (see Bear (Bear, 1988)). In that case a similarity solution can not be obtained. With numerical methods however it is possible to obtain a solution that includes velocity-dependent dispersion.

The non-Boussinesq volume effects are highly increased when velocity-dependent hydrodynamic dispersion is taken into account. This is illustrated in Figure 5, which shows the computed initial specific discharge profile of a one-dimensional heat transfer problem. For simplicity, solute transport is disregarded here. Similar to the examples discussed before, a steep temperature/density gradient at $x = 0$ causes an enhancement of the specific discharge in this region. In contrast to the earlier examples a background flow is considered in this case.

Three lines are shown in Figure 5. The solid line corresponds to the case in which only thermal diffusion is taken into account, where the scaled diffusion coefficient a^* equals 0.04 (corresponding to a porous medium thermal diffusivity of $4.0 \cdot 10^{-7}$ m^2/s). The increase in the specific discharge due to the volume effects is very small compared to the background flow and therefore not visible. In the second case hydrodynamic dispersion is taken into account by taking a much larger but constant diffusion/dispersion coefficient. This coefficient equals ten times the background flow ($q = 1$). The dashed line shows that in this case the discharge is almost doubled around $x = 0$. Because the specific discharge is not constant along x, a realistic dispersion coefficient should not be a constant either. When the diffusion/dispersion coefficient is made velocity-dependent ($a^* = 10q$), the non-Boussinesq effect is strongly increased. This is illustrated by the third line in Figure 5.

When the Boussinesq approximation is adopted, the increase of the specific discharge in the vicinity of $x = 0$ is neglected. Figure 5 shows that the effects can be large. However, the discharge enhancement is a very local effect. Furthermore it

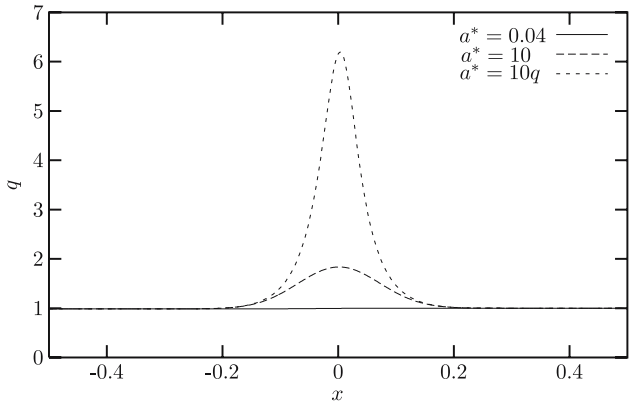

Fig. 5 The enhancement of the specific discharge due to fluid volume changes in a one-dimensional heat transfer problem. Shown are three cases: thermal diffusion only, a constant dispersion coefficient and a velocity-dependent dispersion coefficient

decreases rapidly in time as the gradients that cause it diminish, as a result of the diffusion/dispersion processes.

4.2 Vertical brine displacement in a heterogeneous column

The last example is two-dimensional, and one in which gravity plays an important role. We consider the upward displacement of fresh water by a dense salt solution (brine) in a heterogeneous porous column. Due to the heterogeneous permeability field the velocity field is non-uniform, causing a kind of fingering in the front. We consider the gravitationally stable case, with fresh water on top. Gravity flow, induced by density gradients, is counteracting the growth of dispersive fingers. As a result, the widening of the transition zone is suppressed when significant density gradients are present.

The equations (1), (2), and (4) were solved numerically, using the code d^{3}f (Fein, 1998) for density-dependent flow in porous media. Numerical convergence of the solutions was tested, and will be discussed in detail in a future paper. Micro scale dispersion is incorporated in the model, but the spreading resulting from the variable velocity field is of greater importance ($A_{11} \sim \lambda\sigma^2 = 10^{-3}$ m). The permeability field was assumed to have a log-normal distribution, and was generated based on a Gaussian correlation function, using the random field generator *FGEN* developed by Robin et al. (Robin et al., 1993). In Figure 6 the heterogeneous column is depicted, with the applied boundary conditions. As an illustration, some computed concentration contours for the tracer case are depicted as well. The permeability varies over about one order of magnitude. The essential parameters are given in Table 2. These parameters yield $N\mathrm{Pe} = 92$.

In Figure 7 horizontally averaged concentration profiles are plotted, at the time that corresponds to a travel distance of approximately ninety correlation lengths. Shown are four cases:

1. $\rho_s = 1200,\ g = 9.81$
2. $\rho_s = 1200,\ g = 0$
3. $\rho_s = 1200,\ g = 9.81$, with Boussinesq approximation
4. $\rho_s = 1000$.

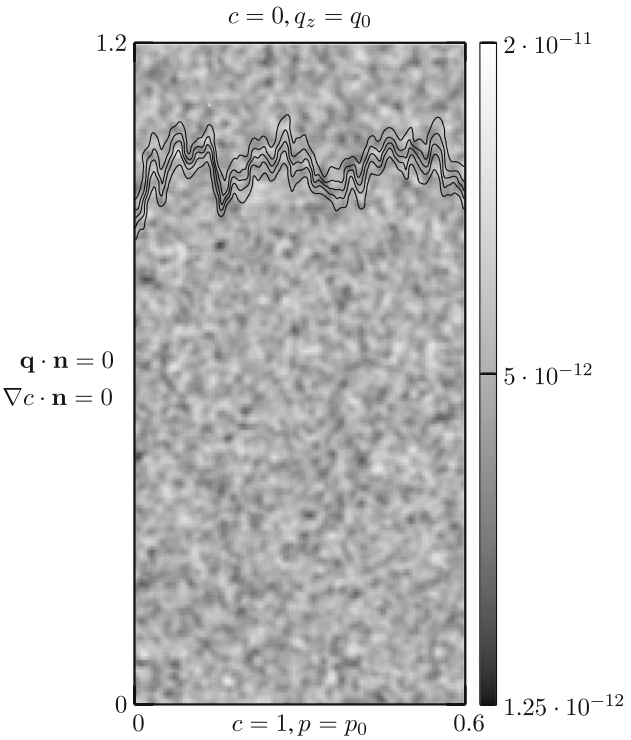

Fig. 6 The heterogeneous porous column, with boundary conditions and concentration contours for a tracer (case 4). The vertical scale bar represents the permeability values in m^2 units

Table 2 Parameters of heterogeneous column

Height	H	1.2	m
Width	W	0.6	m
Correlation length	λ	0.01	m
Average permeability	$\bar{k}$	5.0×10^{-12}	m^2
Ln k variance	$\sigma^2_{\ln k}$	0.1	–
Long. micro scale dispersivity	α_L	1×10^{-4}	m
Transv. micro scale dispersivity	α_T	1×10^{-4}	m
Porosity	n	0.4	–
Mean specific discharge	q_0	0.6×10^{-5}	m/s

The first case takes all the effects of density gradients into account, solving the complete system of equations. The second case leaves out the gravity term, by setting $g = 0$. The third case adopts the Boussinesq approximation, retaining the gravity term but ignoring the effect of volume changes ($\nabla \cdot \mathbf{q} = 0$). The last case neglects all density effects, setting the density of brine equal to that of fresh water.

Comparing case 1 and 2, there is a large difference in the steepness of the profile, purely due to the gravity term. Stabilizing rotational gravity flow reduces the size of the fingers, which are due to the heterogeneous permeability field. This results

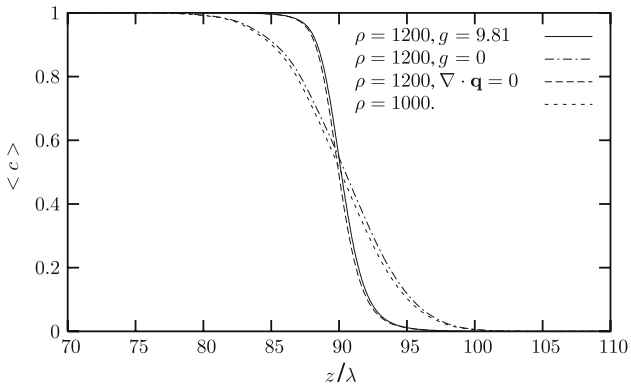

Fig. 7 Concentrations averaged over the width of the heterogeneous column, at an equivalent travel time of $tq_0/n = 90\lambda$

in a smaller transition zone width and a steeper profile of the horizontally averaged concentration.

Comparing case 1 with case 3, the full set of equations and the Boussinesq approximation respectively, illustrates the volume effect. In both cases the gravity term is present, resulting in a similar steepness of the curve. In case 1 however, the curve is shifted compared to that of case 3. This is due to the volume changes that are taken into account and cause an enhancement of the specific discharge at the location of the front. So, with the full set of equations the concentration distribution moves with a slightly higher velocity than with the Boussinesq approximation. The same effect is seen when cases 2 and 4 are compared. In both cases the gravity effect is absent, resulting in more dispersed profiles, but the profile in case 2, which includes the volume effect, is slightly shifted to the right compared to case 4.

In this 2D example gravity played an important role, having a significant effect on the transition zone width between brine and fresh water. Adopting the Boussinesq approximation did not change the shape of the concentration distribution, but only caused a slight shift in it. Even though the volume effect was visible, it was insignificant, the shift being smaller than 0.5% of the travelled distance.

5 Conclusions

In the Boussinesq approximation all density variations are neglected, except for the gravity term in Darcy's law. The limit of vanishing density differences ($\varepsilon \downarrow 0$) is in contradiction with this assumption, because the gravity effect in this limit disappears as well.

Comparing the term accounting for fluid volume changes ($\nabla \cdot \mathbf{q} \neq 0$) with the gravity term in the scaled pressure equation, explains why and when it is justified to neglect the first, while retaining the latter. For isothermal brine transport a condition needs to be fulfilled for a dimensionless number, which is independent of the density difference and characteristic discharge:

$$N\mathrm{Pe} = \frac{\mathrm{Ra}}{\varepsilon} = \frac{kg\rho_0 x_0}{\mu D} \gg 1. \tag{39}$$

For heat transfer in a porous medium two conditions must be met to obtain the equations as in the Boussinesq approximation:

$$N\frac{\mathrm{Pe}}{\mathrm{Le}} = N\mathrm{Pe}_{\mathrm{T}} \gg 1, \quad \text{and } N \gg |\mathbf{q}|. \tag{40}$$

The extra condition involving the specific discharge results from the fact that the solid grains have a heat capacity, causing a retardation.

When transport of both heat and brine is considered, the fluid volume changes that occur are simply a sum of the volume changes caused by the two separate effects. Therefore, to be able to neglect the volume changes compared to the gravity term, the conditions for both cases must be fulfilled.

One-dimensional similarity solutions for simultaneous transport of heat and brine were obtained. These solutions were consistent with those obtained with a numerical method. These diffusion dominated problems (Pe of order ε), illustrate the effect of fluid volume changes on the specific discharge. This effect is neglected when the Boussinesq approximation is adopted, introducing an error that is enlarged when velocity-dependent hydrodynamic dispersion is taken into account.

Due to the one-dimensionality, gravity did not play a role in these examples. To illustrate the relative effects of volume changes and gravity, a two-dimensional example was given, in which fresh water was displaced by brine in a heterogeneous porous column. The effect of fluid volume changes was visible but small, resulting in a slight shift in the concentration distribution. The effect of gravity however was much larger, changing the shape of the concentration distribution significantly. These results, obtained for $N\mathrm{Pe} = 92$, are consistent with condition (39).

Appendix: Similarity solutions

In the following derivation, one-dimensional equations are considered. Darcy's law is not needed to calculate the specific discharge q, since q is treated as an unknown variable. The other two unknowns are the scaled density ρ, and the scaled temperature T. The three equations that need to be solved are the fluid mass balance, salt mass balance and energy balance. We start with the one-dimensional versions of (13)–(15), a system of coupled partial differential equations. This system is transformed into a set of ordinary differential equations using:

$$\eta = \frac{x}{\sqrt{t}}, \quad T(x,t) = f(\eta), \quad \rho(x,t) = u(\eta), \text{ and } q(x,t) = \frac{v(\eta)}{\sqrt{t}}. \tag{41}$$

These substitutions are similar to those used by van Duijn et al. (Duijn et al., 1998), who consider isothermal brine transport in porous media. After rearrangement the three equations become:

$$\varepsilon\left(v - \frac{1}{2}\eta\right)u' + (1+\varepsilon u)v' = 0, \tag{42}$$

$$(1+\varepsilon u)\left(v - \frac{1}{2}\eta\right)f' - \frac{1}{2}A\eta f' - \frac{\mathrm{Le}}{\mathrm{Pe}}f'' = 0, \tag{43}$$

$$\left(v - \frac{1}{2}\eta\right)(\varepsilon u' + \alpha(1+\varepsilon u)f') - \frac{\varepsilon}{\mathrm{Pe}}u'' - \frac{\alpha}{\mathrm{Pe}}((1+\varepsilon u)f')' = 0, \tag{44}$$

where $'$ denotes the derivative with respect to η. Differentiating (43) and rearranging terms yields:

$$\left(\frac{f''}{f'}\right)' = \varepsilon\frac{\mathrm{Pe}}{\mathrm{Le}}\frac{\left(Av + \mathrm{Le}\frac{f''}{f'}\right)u'}{1+\varepsilon u + A} + \frac{\mathrm{Pe}}{\mathrm{Le}}(1+\varepsilon u)v' - 2\frac{\mathrm{Pe}}{\mathrm{Le}}(1+\varepsilon u + A). \tag{45}$$

Substituting (44) into (43) to eliminate η gives an expression for u'':

$$u'' = -\frac{\alpha}{\varepsilon}[(1+\varepsilon u)f']' + \mathrm{Pe}\frac{\varepsilon u' + \alpha(1+\varepsilon u)f'}{\varepsilon(1+\varepsilon u + A)}\left(\mathrm{Le}\frac{f''}{f'} + Av\right). \tag{46}$$

Furthermore, an expression for v' is obtained by combining (42) and (43):

$$v' = \frac{-\varepsilon u'\left(Av + \frac{\mathrm{Le}}{\mathrm{Pe}}\frac{f''}{f'}\right)}{(1+\varepsilon u)(1+\varepsilon u + A)}. \tag{47}$$

Note that (45) is a third order differential equation. This implies that to solve this system of equations a third boundary condition for f is needed. To avoid this problem, a temperature flux y is introduced that reduces the order of (45). Now consider all variables to be functions of f instead of functions of η, which is allowed because f is a monotonous function of η. The advantage of this is that the domain becomes finite. So:

$$y = y(f) = -f'(\eta(f)), \quad u = u(f), \quad v = v(f). \tag{48}$$

All derivatives with respect to η are substituted by derivatives with respect to f using:

$$\frac{d}{d\eta} = \frac{d}{df}\frac{df}{d\eta} = -y\frac{d}{df}. \tag{49}$$

Finally, the following set of equations is obtained:

$$y\frac{d^2y}{df^2} + \frac{\varepsilon}{\mathrm{Le}/\mathrm{Pe}}\frac{Av - \frac{\mathrm{Le}}{\mathrm{Pe}}\frac{dy}{df}}{(1+\varepsilon u + A)}y\frac{du}{df} + \frac{(1+\varepsilon u)}{\mathrm{Le}/\mathrm{Pe}}y\frac{dv}{df} + \frac{1+\varepsilon u + A}{2\mathrm{Le}/\mathrm{Pe}} = 0. \tag{50}$$

$$\begin{aligned}\frac{d}{df}\left(y\frac{du}{df}\right) &+\frac{\alpha}{\varepsilon}\left(\varepsilon y\frac{du}{df} + (1+\varepsilon u)\frac{dy}{df}\right)\\ &-\mathrm{Pe}\frac{\varepsilon\frac{du}{df} + \alpha(1+\varepsilon u)}{\varepsilon(1+\varepsilon u + A)}\left(\frac{\mathrm{Le}}{\mathrm{Pe}}\frac{dy}{df} - Av\right) = 0,\end{aligned} \tag{51}$$

$$\frac{dv}{df} = -\frac{\varepsilon\frac{du}{df}\left(Av - \frac{\mathrm{Le}}{\mathrm{Pe}}\frac{dy}{df}\right)}{(1+\varepsilon u)(1+\varepsilon u + A)}. \tag{52}$$

With appropriate boundary conditions these equations can be solved numerically, e.g. using a standard finite difference scheme. When y, u and v are known as functions of f, the last step is to transform them back to functions of the similarity variable η. Therefore, an additional expression for η in terms of y, u, and v is needed. From (43), (48), and (49) it follows that:

$$\eta = 2\frac{(1+\varepsilon u)v + \frac{\mathrm{Le}}{\mathrm{Pe}}\frac{dy}{df}}{1+\varepsilon u + A}. \tag{53}$$

The initial conditions of problem I as given by (31) correspond to the following conditions for $u(\eta), f(\eta)$, and $v(\eta)$:

$$\begin{aligned} f(-\infty) = 0, \quad u(-\infty) = 1, \\ f(\infty) = 1, \quad u(\infty) = 0, \quad v(\infty) = 0. \end{aligned} \tag{54}$$

Note that for a non-zero background flow at $x \to \infty$ the boundary condition for v becomes a function of time (see (41)). In that case a similarity solution can not be found. For the case of brine transport, this problem can be overcome by decomposing the specific discharge q, into a constant part (the background flow) and a deviation. In addition, the similarity variable is adjusted. Unfortunately, this procedure does not work here, because the temperature profile does not move with the same velocity as the salt mass fraction profile due to thermal retardation. Consequently, a zero background velocity is a necessary choice.

The boundary conditions needed to solve the system (50)–(52) are given by:

$$\begin{aligned} u(0) = 1, \quad u(1) = 0, \\ y(0) = 0, \quad y(1) = 0, \\ v(1) = 0. \end{aligned} \tag{55}$$

In problem II, the initial profile of the salt mass fraction is reversed. As the temperature and mass fraction distributions have opposite effects on the density, the minimum and maximum density are not reached in this case. The conditions for $u(\eta), f(\eta)$, and $v(\eta)$ are:

$$\begin{aligned} f(-\infty) = 0, \quad u(-\infty) = \frac{1}{\varepsilon}(e^{\alpha} - 1), \\ f(\infty) = 1, \quad u(\infty) = \frac{1}{\varepsilon}(e^{\gamma} - 1), \quad v(\infty) = 0. \end{aligned} \tag{56}$$

Note that the maximum temperature difference and salt mass fraction are incorporated in α and γ (see (10)). To obtain the similarity solution for this problem, the system (50)–(52) is solved subject to the following boundary conditions:

$$\begin{aligned} u(0) = \frac{1}{\varepsilon}(e^{\alpha} - 1), \quad u(1) = \frac{1}{\varepsilon}(e^{\gamma} - 1), \\ y(0) = 0, \quad y(1) = 0, \\ v(1) = 0. \end{aligned} \tag{57}$$

References

Bear, J.: Dynamics of Fluids in Porous Media. Dover, New York (1988)
Boussinesq, J.: Théorie Analytique de la Chaleur, vol. 2. Gauthier-Villars, Paris (1903)
Fein E.: D3f - Ein Programmpaket zur Modellierung von Dichteströmungen GRS- 139, Braunschweig, Germany (1998)
Gartling, D.K., Hickox, C.E.: A numerical study of the applicability of the Boussinesq approximation for a fluid-saturated porous medium. International Journal for Numerical Methods in Fluids **5**, 995–1013 (1985)
Gray, D.D., Giorgini, A.: The validity of the Boussinesq approximation for liquids and gases. Int. J. Heat Mass Transfer **19**, 545–551 (1976)
Johannsen, K.: On the validity of the Boussinesq approximation for the Elder problem. Computational Geosciences **7**(3), 169–182 (2003)

Joseph, D.D.: Stability of Fluid Motions II. Springer-Verlag, Berlin (1976)
Leijnse T.: Free convection for high concentration solute transport in porous media. In: Kobus, H.E. and Kinzelbach, W. (eds.) Contaminant Transport in Groundwater, pp. 341–346. Balkema, Rotterdam (1989)
Oberbeck, A.: Über die Wärmeleitung der Flüssigkeiten bei Berücksichtigung der Strömungen infolge von Temperaturdifferenzen. Annalen der Physik und Chemie **7**, 271–292 (1879)
Peirotti, M.B., Giavedoni, M.D., Deiber, J.A.: Natural convective heat transfer in a recangular cavity with variable fluid properties - validity of the Boussinesq approximation. Int. J. Heat Mass Transfer **30**(12), 2571–2581 (1987)
Rajagopal, K.R., Ruzicka, M., Srinivasa, A.R.: On the Oberbeck-Boussinesq approximation. Mathematical Models and Methods in Applied Sciences **6**(8), 1157–1167 (1996)
Robin, M.J.L., Gutjar, A.L., Sudicky, E.A., Wilson, J.L.: Cross-Correlated Random Field Generation With the Direct Fourier Transform Method. Water Resources Research **29**(7), 2385–2397 (1993)
van Duijn, C.J., van Peletier, L.A., Schotting, R.J.: Brine transport in porous media: self-similar solutions. Advances in Water Resources **22**(3), 285–297 (1998)